

# Surface Gloss Reduction of EVA Foam Using Rice Husk-derived Bio-silica with Improved Dispersion via Silane Coupling

Gi-Yong Um<sup>1</sup> and Jun-Ha Jeon<sup>1,\*</sup>

<sup>1</sup> Korea Institute of Materials Convergence Technology, Busan 47154, Republic of Korea.

\*Corresponding Author: juna@kimco.re.kr

**ABSTRACT:** This study investigated the application of rice husk-derived bio-silica as an eco-friendly matting agent to reduce the surface gloss of ethylene-vinyl acetate (EVA) foams. Bio-silica was incorporated at loading levels of 2, 4, 6, 8, and 10phr relative to EVA. While the addition of bio-silica effectively reduced surface gloss, it led to decreased crosslink density, resulting in deteriorated tensile strength and compression set resistance. Poor dispersion of silica particles and agglomeration were observed in the foam structure. To address these issues, a pre-mixing approach using silane coupling agent was employed. The silane-treated bio-silica significantly improved the crosslink density retention and mechanical properties while maintaining the desired matting effect. The pre-treatment method also enhanced silica dispersion within the foam matrix, leading to improved internal foam morphology. This approach demonstrates a viable strategy for developing eco-friendly EVA foams with controlled surface characteristics and balanced physical properties..

**KEY WORDS:** EVA foam, bio-silica, rice husk, surface gloss, matting agent, silane coupling agent, dispersion

Date of Submission: 12-12-2025

Date of acceptance: 24-12-2025

## I. INTRODUCTION

Ethylene-vinyl acetate (EVA) copolymer foams are widely used in footwear applications, particularly in shoe midsoles, due to their excellent cushioning properties, lightweight characteristics, and processing flexibility [1-3]. The aesthetic appearance of EVA foams, particularly surface gloss, is an important factor affecting consumer preference and product differentiation in the competitive footwear market. High-gloss surfaces may appear less natural or premium in certain product segments, driving demand for matte-finish EVA foams [4,5].

Traditionally, synthetic inorganic fillers such as precipitated silica, calcium carbonate, or talc have been used as matting agents to reduce surface gloss [6,7]. However, increasing environmental concerns and consumer demand for sustainable products have prompted the search for eco-friendly alternatives. Rice husk, an agricultural by-product generated in large quantities during rice processing, contains approximately 15-20% silica by weight [8,9]. The extraction of silica from rice husk not only provides a valuable resource but also contributes to waste valorization and circular economy principles.

Bio-silica derived from rice husk has been explored in various rubber and polymer composites due to its high surface area, amorphous structure, and reinforcing potential [10-12]. Adam et al. [10] reported that rice husk silica exhibited similar reinforcing effects to commercial precipitated silica in natural rubber compounds. Shen et al. [11] investigated the incorporation of rice husk ash in styrene-butadiene rubber (SBR) composites and observed improved tensile strength at optimal loading levels. More recently, Kumar et al. [12] demonstrated the potential of functionalized rice husk silica in enhancing the mechanical properties of polyethylene composites.

However, the incorporation of bio-silica into polymer matrices often faces challenges related to filler-polymer compatibility and dispersion. The hydrophilic nature of silica surfaces contrasts with the hydrophobic character of EVA, leading to poor interfacial adhesion and particle agglomeration [13,14]. These issues can negatively impact crosslinking reactions and mechanical properties of the foam. Liu et al. [13] reported that untreated silica fillers formed large agglomerates in polyolefin matrices, acting as stress concentrators and reducing mechanical performance. Similarly, Zhang et al. [14] observed that poor silica dispersion in EVA composites led to non-uniform crosslink density distribution and inferior foam cell morphology.

Silane coupling agents have been widely employed to improve the compatibility between inorganic fillers and organic polymer matrices [15-17]. These bifunctional molecules possess both inorganic-reactive groups (typically alkoxy silanes) and organic-compatible groups, enabling chemical bonding at the filler-polymer interface. Plueddemann [15] pioneered the understanding of silane coupling mechanisms, demonstrating that silanes hydrolyze to form silanol groups that condense with hydroxyl groups on filler surfaces. Rothon [16] comprehensively reviewed the role of coupling agents in filled polymers, emphasizing their importance in stress transfer and interfacial adhesion. Recent work by Xie et al. [17] showed that vinyl-functional silanes significantly improved the dispersion of silica in peroxide-cured rubber compounds, with enhanced crosslink density and mechanical properties.

Despite extensive research on silane-treated silica in various polymer systems, the application of silane coupling agents for rice husk-derived bio-silica in EVA foam systems remains underexplored. Furthermore, the specific challenge of maintaining matting effectiveness while improving mechanical properties through silane treatment has not been systematically investigated. The balance between surface aesthetics and structural performance is critical for commercial footwear applications, where both visual appeal and durability are essential requirements.

This study aims to evaluate the effectiveness of rice husk-derived bio-silica as a sustainable matting agent for EVA foams and to address the associated technical challenges through silane coupling agent pre-treatment. The research investigates the effects of bio-silica loading on crosslinking characteristics, mechanical properties, and surface gloss. An improved processing method using silane pre-treatment is demonstrated to achieve balanced performance with enhanced dispersion, maintained matting effectiveness, and improved mechanical properties.

## **II. Experimental**

### **2.1 Materials**

Ethylene-vinyl acetate copolymer (EVA, trade name: EVA 420, vinyl acetate content: 28%, melt index: 2.5 g/10 min at 190°C) was supplied by LG Chem (Korea). Rice husk-derived bio-silica (specific surface area: 180m<sup>2</sup>/g, average particle size: 8µm, silicon dioxide content: >95%) was obtained from Fenghal Rice Biotechnology (China). Dicumyl peroxide (DCP, 99% purity) was used as the crosslinking agent and was purchased from Sigma-Aldrich. Azodicarbonamide (ADCA, decomposition temperature: 155-160°C, gas yield: 210 mL/g) served as the chemical blowing agent and was obtained from Kumyang (Korea). Vinyltrimethoxysilane (VTMS, 98% purity) was employed as the silane coupling agent and was purchased from Sigma-Aldrich. Zinc oxide (ZnO, 99.5% purity, average particle size: 1µm) and stearic acid (St/A, 95% purity) were obtained from Daejung Chemicals (Korea) and used as activators. All materials were used as received without further purification.

### **2.2 Preparation of EVA Foam Compounds**

#### **2.2.1. Direct Mixing Method**

EVA compounds were prepared using an internal mixer (Brabender Plasticorder, chamber volume: 250cm<sup>3</sup>). EVA resin and bio-silica (at loading levels of 0, 2, 4, 6, 8, and 10phr), along with zinc oxide (5phr) and stearic acid (1phr), were charged into the mixer at 80°C and mixed for 10 minutes at a rotor speed of 60 rpm. After mixing, the compound was discharged and allowed to cool to room temperature. The cooled compound was then transferred to a two-roll mill operating at 80°C. The crosslinking agent (dicumyl peroxide, DCP) and blowing agent (azodicarbonamide, ADCA) were incorporated into the compound by adding them gradually over 5 minutes while passing the material through the mill rolls. The addition of these temperature-sensitive components on the two-roll mill rather than in the internal mixer prevented premature decomposition and ensured processing safety. The final compound was sheeted to approximately 3 mm thickness and allowed to rest for 24 hours at room temperature before foam molding.

#### **2.2.2. Silane Pre-treatment Method**

For the silane-treated samples, bio-silica was first dried in a vacuum oven at 110°C for 2 hours to remove moisture, which is critical for effective silane reaction. The dried bio-silica, vinyltrimethoxysilane (10wt% relative to silica), and EVA resin were charged into the internal mixer at 140°C. The mixture was processed for 10 minutes at 100 rpm to ensure adequate time for silane hydrolysis and condensation reactions with silica surface hydroxyl groups. The elevated mixing time compared to the direct method allowed complete silane reaction and improved silica dispersion in the polymer matrix. After mixing, the compound was discharged and

allowed to cool to room temperature. The cooled silane pre-treatment compounds processed on the internal mixer and two-roll mill following the same procedure as the direct mixing method.

### **2.3 Foam Molding**

The prepared compounds were compression molded using a hydraulic press equipped with temperature control. Heating was conducted at 170°C for 10 minutes under a pressure to ensure foaming and crosslinking. The mold was then opened, and the compound was allowed to expand to achieve the desired foam structure. The foaming temperature was selected based on the decomposition profile of ADCA. After foaming, the samples were removed from the mold and cooled to room temperature under ambient conditions. The resulting foam sheets were conditioned at 23°C and 50% relative humidity for 24 hours before testing.

### **2.4 Characterization**

#### **2.4.1. Crosslinking Characteristics**

Oscillating disc rheometry (ODR) was performed using a Moving Die Rheometer (MDR 2000, Alpha Technologies) at 170°C for 20 minutes according to ASTM D2084. Approximately 5 g of uncured compound was placed in the die cavity, and the torque was measured as a function of time. The following parameters were recorded: maximum torque ( $M_H$ ), minimum torque ( $M_L$ ), torque difference ( $M_H - M_L$ , which is proportional to crosslink density), scorch time ( $t_{s2}$ , time to 2% torque rise), and optimum cure time ( $t_{90}$ , time to reach 90% of maximum torque). All tests were performed in duplicate, and average values were reported.

#### **2.4.2. Physical and Mechanical Properties**

Hardness was measured using a Type C durometer according to ASTM D2240. Measurements were taken at five different locations on each foam sample, and the average value was reported.

Tensile properties were evaluated using dumbbell-shaped specimens (Type 3, ASTM D412) die-cut from foam sheets. Tests were conducted on a universal testing machine (Instron 5966) at a crosshead speed of 500 mm/min and a gauge length of 20 mm. Tensile strength, elongation at break, and modulus at 100% elongation ( $M_{100}$ ) were recorded. Five specimens were tested for each formulation, and average values with standard deviations were calculated.

Compression set was determined at 50°C for 6 hours under 50% deflection according to ASTM D395. Cylindrical specimens (diameter: 15mm, thickness: 10mm) were compressed between parallel plates in a compression set fixture and placed in an air-circulating oven. After the test period, samples were removed from the fixture, allowed to recover for 30 minutes at room temperature, and the final thickness was measured. Compression set percentage was calculated as:  $CS (\%) = [(t_0 - t_f) / (t_0 - t_s)] \times 100$ , where  $t_0$  is original thickness,  $t_f$  is final thickness after recovery, and  $t_s$  is spacer bar thickness. Three specimens were tested per formulation.

#### **2.4.3. Surface Gloss Measurement**

Surface gloss was measured at 60° angle using a tri-angle gloss meter (BYK-Gardner micro-TRI-gloss  $\mu$ ) according to ASTM D523. The 60° geometry is standard for materials with medium gloss levels. Measurements were taken at five different locations on the foam surface, avoiding areas near edges and any visible defects. The instrument was calibrated using a certified gloss standard before each measurement session. Results were reported as gloss units (GU) with average values and standard deviations.

## **III. RESULTS AND DISCUSSIONS**

### **3.1 Material Effect of Bio-silica on Surface Gloss**

Figure 1 shows the effect of bio-silica loading on the surface gloss of EVA foams prepared by the direct mixing method. The control EVA foam (0phr bio-silica) exhibited a surface gloss of 25.2GU, characteristic of conventional compression-molded EVA foams. The addition of bio-silica progressively reduced the surface gloss, with values of 18.7GU (2phr), 12.4GU (4phr), 9.8GU (6phr), 6.5GU (8phr), and 3.3GU (10phr). At the highest loading level, surface gloss was reduced by 86% compared to the control, achieving a distinctly matte appearance.

This matting effect can be attributed to the increased surface roughness and light scattering caused by the silica particles at the foam surface. During compression molding, silica particles migrate toward the mold surfaces and protrude slightly from the polymer matrix, creating microscale surface irregularities. The

amorphous structure and high surface area of bio-silica ( $180\text{m}^2/\text{g}$ ) contribute to effective light diffusion. Unlike specular reflection from smooth surfaces, the roughened surface scatters incident light in multiple directions, reducing the intensity of reflected light detected by the gloss meter. The effectiveness of silica as a matting agent has been previously reported in coating and polymer systems, where surface roughness is the primary mechanism for gloss reduction [6,7].

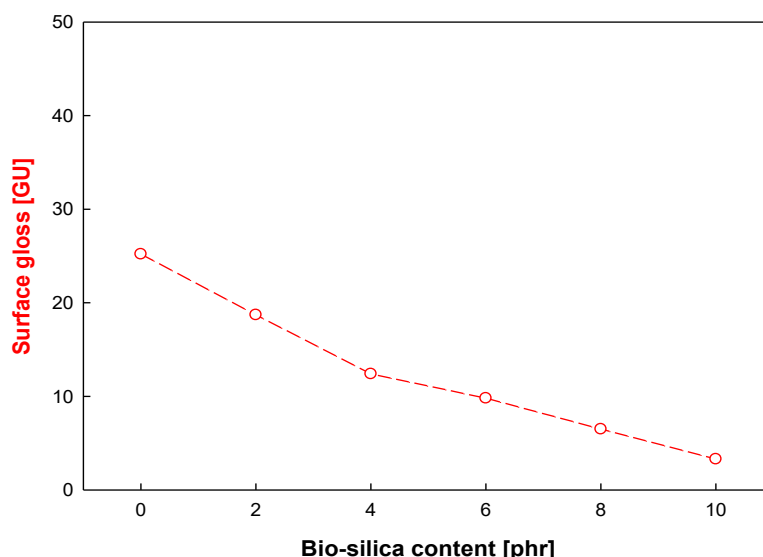


Figure 1. Variation in the surface gloss of EVA foams depending on bio-silica content

### 3.2 Crosslinking Characteristics

Table 1 presents the ODR results for EVA compounds with varying bio-silica contents prepared by the direct mixing method. The incorporation of bio-silica led to a systematic decrease in crosslink density, as evidenced by the reduction in torque difference ( $M_H - M_L$ ). For the control sample (0phr),  $M_H - M_L$  was 0.32Nm. This value decreased to 0.24Nm (2phr), 0.17Nm (4phr), 0.14Nm (6phr), 0.12Nm (8phr), and 0.10Nm (10phr), representing a 68% reduction at the highest loading level.

This phenomenon can be explained by several synergistic factors. First, the high surface area of bio-silica ( $180\text{ m}^2/\text{g}$ ) provides abundant sites for physical or chemical adsorption of dicumyl peroxide. The surface silanol groups (Si-OH) can form hydrogen bonds with the carbonyl groups of DCP, effectively reducing the concentration of free peroxide available for EVA crosslinking. This adsorption effect has been reported for other peroxide-filler systems [18,19]. Second, silica particles can physically interfere with the propagation of radical reactions during peroxide decomposition. The generated radicals (cumyloxy radicals from DCP) must diffuse through the polymer matrix to abstract hydrogen atoms from EVA chains. The presence of inert silica particles increases the tortuosity of diffusion paths and reduces the probability of successful radical-polymer encounters. Third, the dilution effect of the non-reactive filler reduces the local concentration of polymer chains, thereby decreasing the probability of intermolecular crosslinking reactions. Finally, the strong particle-particle interactions of untreated hydrophilic silica lead to agglomeration, creating filler-rich and polymer-rich regions. In filler-rich regions, the effective polymer concentration is further reduced, exacerbating the decline in crosslink density.

The optimum cure time ( $t_{90}$ ) slightly increased with bio-silica content, from 6.92minutes (control) to 7.42minutes (10phr), suggesting slower crosslinking kinetics.

**Table 1.**The ODR results of EVA compounds according to bio-silica content

	Bio-silica content [phr]					
	0	2	4	6	8	10
<b>t<sub>90</sub> [Min.]</b>	6.92	7.08	7.12	7.21	7.37	7.42
<b>t<sub>s2</sub> [Min.]</b>	1.06	1.07	1.14	1.20	1.28	1.42
<b>M<sub>H</sub> [Nm]</b>	0.36	0.27	0.20	0.16	0.14	0.10
<b>M<sub>L</sub> [Nm]</b>	0.04	0.03	0.03	0.02	0.02	0.02
<b>M<sub>H</sub>- M<sub>L</sub> [Nm]</b>	0.32	0.24	0.17	0.14	0.12	0.08

### 3.3 Mechanical Properties

Table 2 presents the mechanical properties of EVA foams depending on bio-silica. Figure 2 illustrates the effect of bio-silica loading on tensile properties. Tensile strength decreased progressively from 2.85MPa for the control sample to 2.68MPa (2phr), 2.43MPa (4phr), 2.12MPa (6phr), 1.76MPa (8phr), and 1.48MPa (10phr), representing a 48% reduction at maximum loading. Elongation at break showed a similar declining trend, decreasing from 425% (control) to 398(2phr), 362(4phr), 318% (6phr), 268% (8phr), and 227% (10phr). These mechanical property deteriorations correlate strongly with the reduced crosslink density observed in ODR analysis. In foam materials, the polymer matrix between cells bears the applied stress. The crosslinked network provides elastic recovery and structural integrity. When crosslink density decreases, the network becomes less effective at distributing stress, leading to premature failure at lower stress levels. Additionally, the poor interfacial adhesion between hydrophilic bio-silica and hydrophobic EVA prevents effective stress transfer from the matrix to the filler. Instead of acting as reinforcing agents, poorly bonded silica particles become stress concentration sites where cracks can initiate and propagate.

Hardness measurements (Figure 3) showed a slight increase with bio-silica content, from 58 Shore C (control) to 62 Shore C (10phr). This modest increase is attributed to the rigid filler effect, where hard silica particles resist indentation. However, this increase in surface hardness is insufficient to compensate for the substantial losses in tensile properties and does not indicate improved overall mechanical performance.

Compression set results (Figure 4) revealed a significant deterioration in elastic recovery with increasing bio-silica content. The control sample exhibited a compression set of 52%, indicating excellent shape recovery. This increased to 54% (2phr), 60% (4phr), 68% (6phr), 75% (8phr), and 82% (10phr). A compression set value above 60% is generally considered unacceptable for footwear midsole applications, as it indicates poor long-term cushioning performance. The elevated compression set results from the combination of lower crosslink density and poor filler-matrix interaction. During compression, the weakly bonded silica particles can slip within the matrix, and the under-crosslinked polymer network cannot fully recover its original dimensions. This permanent deformation is detrimental for applications involving repeated loading-unloading cycles, as occurs during walking or running.

**Table2.**The mechanical properties of EVA foams according to bio-silica content

	Bio-silica content [phr]					
	0	2	4	6	8	10
<b>Tensile strength [MPa]</b>	2.85	2.68	2.43	2.12	1.76	1.48
<b>Elongation [%]</b>	425	398	362	318	268	227
<b>Hardness [Shore C]</b>	58	58	59	60	61	62
<b>Compression set [%]</b>	52	54	60	68	75	82

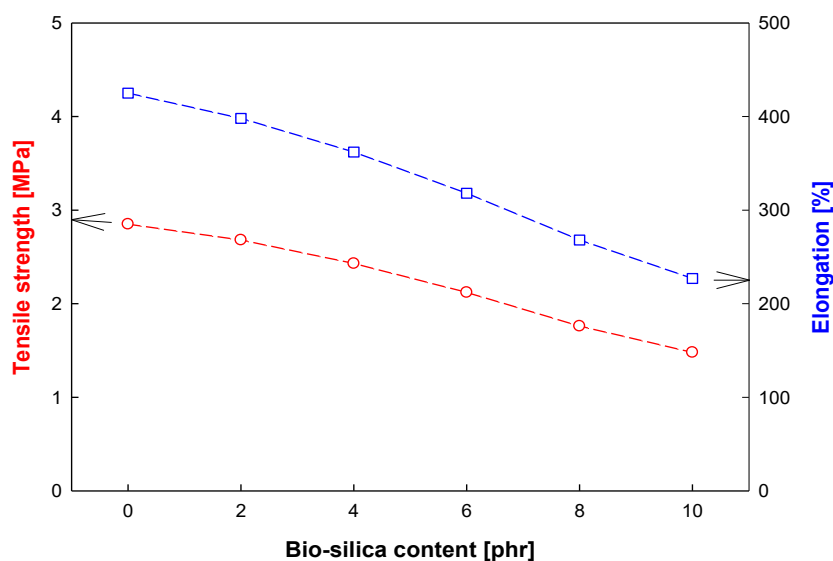


Figure 2. Variation in the tensile properties of EVA foams depending on bio-silica content

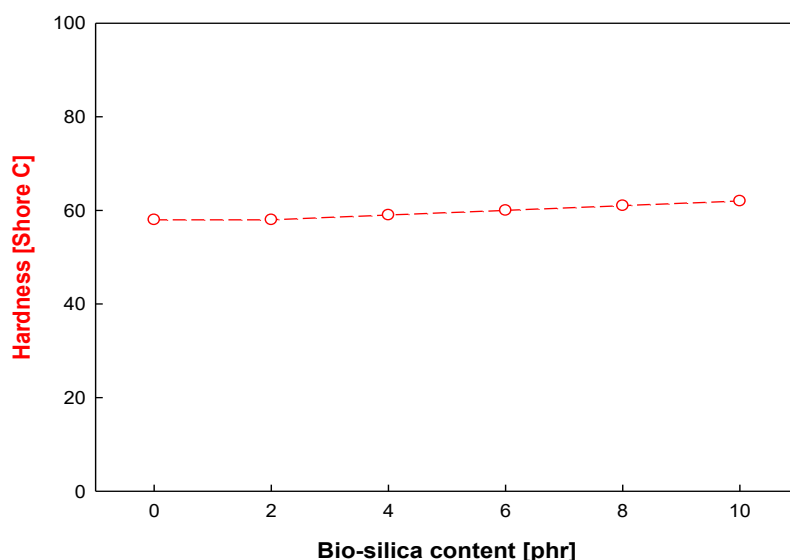


Figure 3. Variation in the hardness of EVA foams depending on bio-silica content

### 3.4 Foam Morphology of Direct-Mixed Samples

Examination of the internal foam structure (Figure 5) indicated notable dispersion deficiencies in samples prepared via direct mixing, with evident bio-silica agglomeration. The resulting aggregates showed irregular shapes and limited interfacial compatibility with the polymer matrix

### 3.5 Improvement via Silane Pre-treatment

#### 3.5.1. Crosslinking Characteristics of Silane-Treated Samples

Table 3 compares the crosslinking properties of EVA foams prepared with silane-treated bio-silica. The pre-treatment approach significantly mitigated the crosslink density reduction observed in direct mixing. At 2phr loading, the  $M_H-M_L$  value for silane-treated samples was 0.31Nm compared to 0.24Nm for directly mixed samples. This improvement became more pronounced at higher loadings: 0.29Nm vs. 0.17Nm (4phr), 0.26Nm vs. 0.14Nm (6phr), 0.22Nm vs. 0.12Nm (8phr), and 0.16Nm vs. 0.08Nm (10phr). At 10phr loading, the silane-



treated sample retained 68% of the control's crosslink density compared to only 50% for the directly mixed sample, representing a 18% improvement in crosslink density retention.

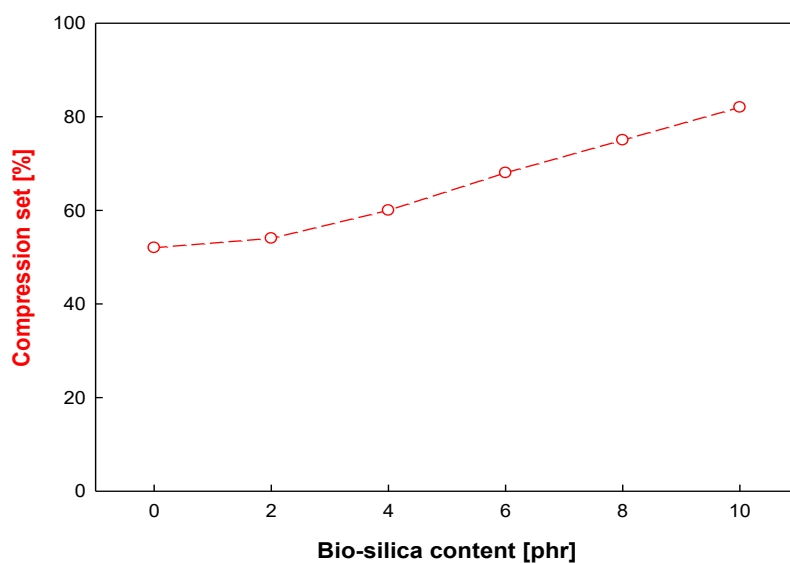


**Figure 4. Variation in the compression set of EVA foams depending on bio-silica content**



**Figure 5. Variation in the internal foam structure of EVA foams depending on bio-silica content**

**Table3.The ODR results of EVA compounds according to silane treated bio-silica content**

	Silane treated bio-silica content [phr]					
	0	2	4	6	8	10
<b>t<sub>90</sub> [Min.]</b>	6.92	6.99	7.06	7.18	7.29	7.42
<b>t<sub>52</sub> [Min.]</b>	1.06	1.07	1.14	1.18	1.22	1.42
<b>M<sub>H</sub> [Nm]</b>	0.36	0.34	0.32	0.28	0.24	0.18
<b>M<sub>L</sub> [Nm]</b>	0.04	0.03	0.03	0.02	0.02	0.02
<b>M<sub>H</sub>- M<sub>L</sub> [Nm]</b>	0.32	0.31	0.29	0.26	0.22	0.16

### 3.5.2. Mechanical Properties of Silane-Treated Samples

The silane-treatment resulted in substantial improvements in mechanical properties (Table 4). At 10phr bio-silica loading, tensile strength increased from 1.48MPa (direct mixing) to 2.24MPa (silane-treatment), representing a 51% improvement and retaining 78% of the control sample's strength. Elongation at break improved from 227% to 352%, approaching 83% of the control value.

Most notably, compression set performance showed dramatic improvement. At 10phr loading, compression set decreased from 82%(direct mixing) to 59%(silane-treatment). This value is within the acceptable range for footwear applications (<60%) and represents a significant achievement in maintaining elastic recovery despite high filler loading.

**Table4.The mechanical properties of EVA foams according to silane treated bio-silica content**

	Silane treated bio-silica content [phr]					
	0	2	4	6	8	10
<b>Tensile strength [MPa]</b>	2.85	2.81	2.75	2.58	2.45	2.24
<b>Elongation [%]</b>	425	415	402	388	369	352
<b>Hardness [Shore C]</b>	58	59	60	62	64	65
<b>Compression set [%]</b>	52	52	54	56	57	59

### 3.5.3. Morphology of Silane-Treated Samples

Examination of the internal foam images of silane-treated samples (Figure 6) demonstrated markedly improved bio-silica dispersion compared to directly mixed samples. Silica agglomeration was significantly reduced.

### 3.5.4. Surface Gloss of Silane-Treated Samples

Importantly, the silane-treatment did not compromise the matting effectiveness of bio-silica (Figure 7). Surface gloss values for pre-treated samples remained comparable to directly mixed samples at equivalent loading levels: 18.7GU vs. 17.9GU (2phr), 12.4GU vs. 12.6GU (4phr), 9.8GU vs. 10.6GU (6phr), 6.5GU vs. 6.2GU (8phr), and 3.3GU vs. 3.0GU (10phr). These minimal differences (within experimental error) indicate that the matting mechanism is preserved with silane treatment. The surface roughness created by silica particles protruding from the mold surface remains effective regardless of the silane modification, as the surface topography is the primary determinant of gloss reduction rather than the chemical nature of the silica surface.





**Figure 6. Variation in the internal foam structure of EVA foams depending on silane-treated bio-silica content**

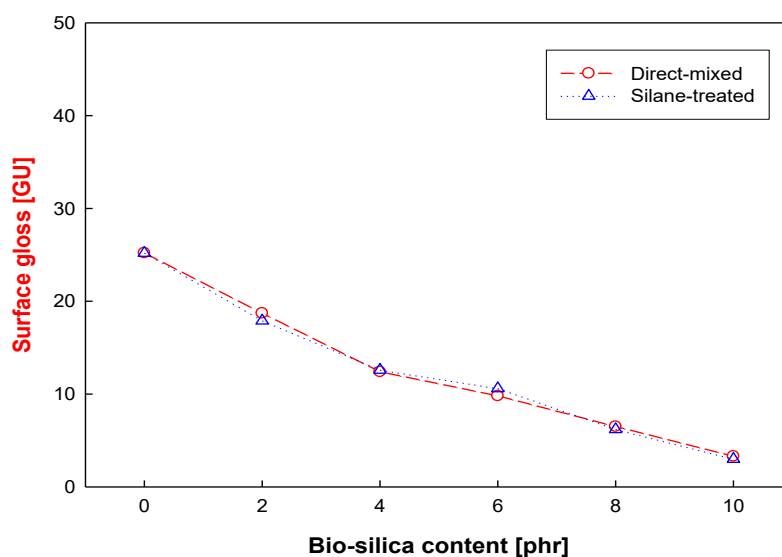


**Figure 7. Variation in the surface gloss of EVA foams depending on bio-silica content and compounding process**

#### IV. CONCLUSIONS AND RECOMMENDATIONS

This study successfully demonstrated the application of rice husk-derived bio-silica as an eco-friendly matting agent for EVA foams, with key findings as follows:

- (1) Bio-silica effectively reduced surface gloss of EVA foams in a dose-dependent manner, with a 62% reduction achieved at 10phr loading. The matting effect is attributed to increased surface roughness and light scattering caused by silica particles at the foam surface.
- (2) Direct incorporation of bio-silica without surface treatment led to several detrimental effects: (a) decreased crosslink density due to peroxide adsorption and dilution effects, (b) compromised tensile strength and elongation at break, (c) deteriorated compression set resistance exceeding acceptable limits at high loading levels, and (d) poor silica dispersion with pronounced agglomeration in the foam structure.
- (3) Pre-treatment of bio-silica with vinyltrimethoxysilane coupling agent in the internal mixer significantly improved performance across multiple metrics: (a) crosslink density retention improved by 18% at 10phr loading, (b) tensile strength increased by 51%, maintaining 78% of control sample strength, (c) compression set was improved, returning to acceptable levels for footwear applications, and (d) silica dispersion was dramatically enhanced.
- (4) The matting effect was fully preserved with silane pre-treatment, as surface gloss values remained statistically equivalent to directly mixed samples at all loading levels. This demonstrates that aesthetic requirements and mechanical performance can be simultaneously achieved through appropriate surface modification.

This research provides a practical and scalable approach for developing sustainable EVA foams with controlled surface characteristics suitable for footwear and other applications. The use of agricultural waste-derived bio-silica addresses environmental concerns while the silane pre-treatment method ensures acceptable mechanical performance.

#### ACKNOWLEDGMENTS

The author(s) disclosed receipt of the following financial support for the research, authorship, and/or publication of this article: This work was supported by Busan Metropolitan City, Republic of Korea (B-2025-01).

#### REFERENCES

- [1]. Kim, S.H., Park, Y.B., Lee, J.W. EVA foam composites for footwear applications: A review of material properties and processing technologies. *Polymer Reviews***2019**, 59, 425-458.
- [2]. Henderson, A.M. Ethylene-vinyl acetate (EVA) copolymers: A general review. *IEEE Electrical Insulation Magazine***1993**, 9(1), 30-38.
- [3]. Rodriguez-Perez, M.A., Simoes, R.D., Constantino, C.J.L., de Saja, J.A. Structure and physical properties of EVA foams containing two types of blowing agents. *Polymer Engineering and Science***2011**, 51, 2245-2256.
- [4]. Chen, L., Wang, Y., Zhang, M. Surface modification strategies for polymer composites: Effects on gloss and appearance properties. *Progress in Organic Coatings***2018**, 124, 88-98.
- [5]. Kobayashi, M., Takahashi, H. Matting agents for polymer surface modification: Mechanisms and applications. *Journal of Applied Polymer Science***2016**, 133, 43254.
- [6]. Wypych, G. *Handbook of Fillers*, 4th ed.; ChemTec Publishing: Toronto, Canada, **2016**.
- [7]. Rotheron, R.N. *Particulate-Filled Polymer Composites*, 2nd ed.; Rapra Technology: Shawbury, UK, **2003**.
- [8]. Kalapathy, U., Proctor, A., Shultz, J. A simple method for production of pure silica from rice hull ash. *Bioresource Technology***2000**, 73, 257-262.
- [9]. Shen, Y. Rice husk silica-derived nanomaterials for sustainable applications. *Renewable and Sustainable Energy Reviews***2017**, 80, 453-466.
- [10]. Adam, F., Appaturi, J.N., Iqbal, A. The utilization of rice husk silica as a catalyst: Review and recent progress. *Catalysis Today***2012**, 190, 2-14.
- [11]. Shen, J., Liu, Z., Li, J., Niu, J. Abrasion resistance and thermal stability of in situ synthesized SiO<sub>2</sub> in styrene-butadiene rubber. *Materials Science and Engineering: A***2008**, 475, 290-296.
- [12]. Kumar, N., Mireja, S., Khandelwal, V., Arun, B., Manik, G. Light-weight high-strength hollow glass microspheres and bamboo fiber based hybrid polypropylene composite: A strength analysis and morphological study. *Composites Part B: Engineering***2017**, 109, 277-285.
- [13]. Liu, X., Wu, Q. Non-isothermal crystallization behaviors of polyamide 6/clay nanocomposites. *European Polymer Journal***2002**, 38, 1383-1389.
- [14]. Zhang, Y., Lee, S., Yoonessi, M., Liang, K., Pittman Jr., C.U. Phenolic resin trapping of mercapto-functional POSS for Fe<sub>3</sub>O<sub>4</sub>-epoxy nanocomposites: Magnetic and thermal properties. *Polymer***2006**, 47, 2984-2996.
- [15]. Plueddemann, E.P. *Silane Coupling Agents*, 2nd ed.; Plenum Press: New York, USA, **1991**.
- [16]. Rotheron, R.N. Effects of particulate fillers on flame retardant properties of composites. In *Particulate-Filled Polymer Composites*; Rotheron, R.N., Ed.; Rapra Technology: Shawbury, UK, **2003**; pp. 263-302.
- [17]. Xie, Y., Hill, C.A.S., Xiao, Z., Militz, H., Mai, C. Silane coupling agents used for natural fiber/polymer composites: A review. *Composites Part A: Applied Science and Manufacturing***2010**, 41, 806-819.
- [18]. Papirer, E., Perrin, J.M., Siffert, B., Philipponneau, G. Surface characteristics of aluminas in relation with polymer adsorption. *Journal of Colloid and Interface Science***1991**, 144, 263-270.
- [19]. Datta, R.N., Ingham, A.R. Thermogravimetric and mass spectrometric studies of vulcanizate degradation: IV. Influence of age-resisting and non-staining antioxidants. *Thermochimica Acta***1990**, 167, 153-166.